Molecular Therapy
Nucleic Acids
Original Article

Change of intracellular calcium level causes acute neurotoxicity by antisense oligonucleotides via CSF route

Chunyan Jia,[1,2,4] Su Su Lei Mon,[1,2,3,4] Ying Yang,[1,2] Maho Katsuyama,[1,2] Kie Yoshida-Tanaka,[1,2] Tetsuya Nagata,[1,2,3] Kotaro Yoshioka,[1,2,3] and Takanori Yokota[1,2,3]

[1]Department of Neurology and Neurological Science, Graduate School of Medical and Dental Sciences, Tokyo Medical and Dental University, Tokyo 113-8519, Japan; [2]Center for Brain Integration Research, Tokyo Medical and Dental University, Tokyo 113-8519, Japan; [3]NucleoTIDE and PepTIDE Drug Discovery Center, Tokyo Medical and Dental University, Tokyo 113-8519, Japan

Antisense oligonucleotides (ASOs) are promising therapeutics for intractable central nervous system (CNS) diseases. For this clinical application, neurotoxicity is one of the critical limitations. Therefore, an evaluation of this neurotoxicity from a behavioral perspective is important to reveal symptomatic dysfunction of the CNS and elucidate the underlying molecular mechanism. We here exploited a behavioral analysis method to categorize and quantify the acute neurotoxicity of mice administered with toxic ASOs via intracerebroventricular injection. The toxic ASOs were found to reduce consciousness and locomotor function in mice in a dose-dependent manner. Mechanistically, we analyzed the effects of modulators against receptors or channels, which regulate calcium influx of neurons, on the ASO neurotoxicity. Modulators promoting calcium influx mitigated, whereas those hindering calcium influx increased, *in vivo* neurotoxicity of ASOs in mice. In an *in vitro* assay to evaluate intracellular free calcium levels using rat primary cortical neurons, toxic ASOs reduced the calcium levels. The findings of this study demonstrated the behavioral characteristics of ASO-induced neurotoxicity and revealed that changes in intracellular free calcium levels are a part of the mechanism underlying the neurotoxic effects of ASO.

INTRODUCTION

Antisense oligonucleotides (ASOs) are synthetic single-stranded DNA or RNA sequences that can hybridize with target RNAs in a Watson-Crick manner and thereby alter the processing of the RNAs to modulate protein production.[1,2] Because the charge and size of ASOs make it very difficult for them to cross the blood-brain barrier, they have been developed to treat central nervous system (CNS) disease by direct injection into cerebrospinal fluid (CSF) space via intrathecal injection.[1-4] Nusinersen, an intrathecally administered drug developed to treat spinal muscular atrophy via intrathecal administration, was the first US Food and Drug Administration (FDA)-approved ASO drug for CNS disease treatment, and it is now marketed in over 40 countries.[5-8] In addition, the drug milasen, which was personalized for a patient with Batten disease named Mila, was designed to correct abnormal mutations in the brain following intrathecal injection by Yu and colleagues[9] and successfully approved by the FDA as a therapeutic for one person, i.e., as an "N-of-1" therapy. This breakthrough in "N-of-1" medication led to further initiatives in various countries to develop patient-customized ASOs.[8,10] The CNS is an ideal target tissue when using this approach because infrequent dosing is feasible via local injection into the CSF space.[8]

To reach the goal of these therapeutics targeting the CNS via the intrathecal route, the neurotoxicity of ASOs in the CNS must be addressed, especially for "N-of-1" ASO drugs because the development period and budget for identifying a safe candidate ASO can be limited.[10] There are several papers showing the characteristics of ASO-induced behavioral abnormalities in the CNS with intrathecal injection.[11-14] In particular, Hagedorn et al.[14] have found that *in vitro* assay measuring calcium oscillations in rat primary neuronal cells can predict the *in vivo* neurotoxicity of mice administered with intracerebroventricular (i.c.v.) injection of ASOs.[13,14] In contrast, molecular pathways underlying this neurotoxicity induced by ASOs remain unclear, and current strategies for preventing the toxicity are insufficient.

Calcium ions play a crucial role in regulating physiological neuronal activities; thus, dysregulation of calcium homeostasis, both extracellularly and intracellularly, can lead to dysfunction of neuronal cells and even neuronal death. On the plasma membrane of neurons, numerous Ca^{2+} channels are activated by ligands with the membrane receptors; the most prominent ligand and widespread excitatory

Received 15 July 2022; accepted 20 December 2022;
https://doi.org/10.1016/j.omtn.2022.12.010.

[4]These authors contributed equally

Correspondence: Kotaro Yoshioka, Department of Neurology and Neurological Science, Graduate School of Medical and Dental Sciences, Tokyo Medical and Dental University, 1-5-45 Yushima, Bunkyo-ku, Tokyo 113-8519, Japan.
E-mail: kotanuro@tmd.ac.jp
Correspondence: Takanori Yokota, Department of Neurology and Neurological Science, Graduate School of Medical and Dental Sciences, Tokyo Medical and Dental University, 1-5-45 Yushima, Bunkyo-ku, Tokyo 113-8519, Japan.
E-mail: tak-yokota.nuro@tmd.ac.jp

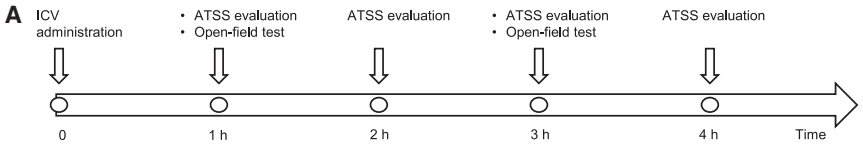

B Acute toxicity scoring system

		Score 1	Score 2	Score 3	Score 4
Category 1 Consciousness	Decreased exploration or involuntary movement	Decreased exploration	Decreased exploration	No exploration	No exploration
	Decreased responsiveness	Normal	Slightly (e.g., reduced response to touch or handling)	Moderately (e.g., reduced response to lift, no blink)	Marked (e.g., reduced response to a tail pinch)
Category 2 Motor function	Ataxia	(-)	Mild (e.g., slow righting response, swaying)	Moderate (e.g., staggering, impaired walking)	Severe (e.g., crawling)
	Strength	Decreased strength of lower limbs	No ability to climb a slope	No ability to walk	No ability to right
Category 3 Appearance	Abnormal posture	Slight	Mild (e.g., hunched, extended, low posture, straub tail)	Moderate (e.g., ventral recumbency)	Severe (e.g., lateral recumbency)
	Abnormal breathing	Normal	Normal	Shallow	Labored
Category 4 Hyperactivity	Increased home-cage exploration	Slightly increased (e.g., increased exploration)	Increased (e.g., digging, burying)	Moderately increased (e.g., scratching limbs)	Marked increased
	Stereotype	(-)	Slight (e.g., increased grooming)	Moderate (e.g., circling, repetitive behavior)	Marked
Category 5 Involuntary movement	Tremors	Detectable	Marked	N.A.	N.A.
	Seizure (e.g., running, bouncing, clonic and/or tonic seizures)	(-)	(-)	Few or partial	Repeated or continuous (e.g., >1 min)
Death	Score 22				

Figure 1. Assessment methods used to characterize and quantify behavioral dysfunction of mice for analysis of ASO-induced neurotoxicity

Experimental design of the neurotoxicity assessment study. (A) Time course of the study. The time course begins with i.c.v. administration of ASO into the left ventricle of the mouse. (B) Acute toxicity scoring system. N.A., not applicable.

transmitter in the CNS is L-glutamate. Inotropic glutamate receptors that mediate calcium ion influx mainly comprise α-amino-3-hydroxy-5-methyl-4-isoxazolepropionic acid receptors (AMPARs) and *N*-methyl-D-aspartate receptors (NMDARs). Importantly, direct interactions between nucleotides, especially guanine nucleotides, and the ionotropic glutamate receptors are well established.[15-21] In addition, Olson et al.[13,14] found that neurotoxic ASOs mediate Ca^{2+} oscillation in cultured neurons. Thus, we hypothesized that a potential mechanism of CNS toxicity by intrathecally injected ASO *in vivo* was mediated by an imbalance in calcium homeostasis and subsequent induction of CNS toxicity.

In the present study, we first assessed symptomatic dysfunction as a result of CNS toxicity in mice administered with ASOs via i.c.v. injection. To this end, we used a behavioral rating scale and assessed locomotor activity in an open-field test. To reveal the mechanism of neurotoxicity, we then tested whether the additional administration modulators targeting receptors or channels associated with calcium dynamics affected the toxic profiles of ASOs *in vivo*. Consequently, we found that an AMPAR antagonist potentiated CNS toxicity, whereas calcium channel activator and AMPAR agonist mitigated this toxicity. In addition, an *in vitro* assay of intracellular free calcium ions with rat primary neuron culture demonstrated that toxic ASOs reduced intracellular free calcium levels. Overall, these findings provide new insights demonstrating the molecular mechanisms underlying ASO neurotoxicity, which involve decreased intracellular free calcium levels in neuronal cells, thereby resulting in acute CNS toxicity.

RESULTS

Phenotypic analysis of acute CNS toxicity caused by ASOs with different structures and target genes

To investigate the phenotypes of CNS toxicity induced by ASOs via the CSF route, we injected three types of ASO (ASO1–3; see Table S1 for details) with different structures and target genes into mice by i.c.v. route. After the injections, mice showed abnormal neurological behaviors, including a decreased desire to explore their cage, reduced responsiveness to stimulation, injured motor function, unusual postures, and disrupted breathing patterns (Video S1). Using the protocol shown in Figure 1A, we scored these abnormal behaviors using acute toxicity scoring system (ATSS) (Figure 1B) from 1 to 4 h after the injection of ASOs. For all three ASOs, neurotoxicity mainly manifested in mice as abnormalities in the categories 1–3, which reflect hypoactivity of consciousness and motor function rather than phenotypes based on the category 4 or 5, which are related to hyperactivities of neurological functions (Figure 2A).

We then assessed the exploration activities and locomotor function of mice using an open-field test. Consistent with the acute tolerability scores, all track plots of mice in the three ASO treatment groups revealed significantly decreased locomotor activity in the open-field arena compared with that of mice in the negative control group, which were injected with phosphate buffer saline (PBS) (Figure 2B). Analysis of the movement parameters, including the total distance traveled, mobile time, and maximum speed, indicated a significant reduction in all three ASO treatment groups compared with the respective parameters in the PBS control group (Figures 2C–2E

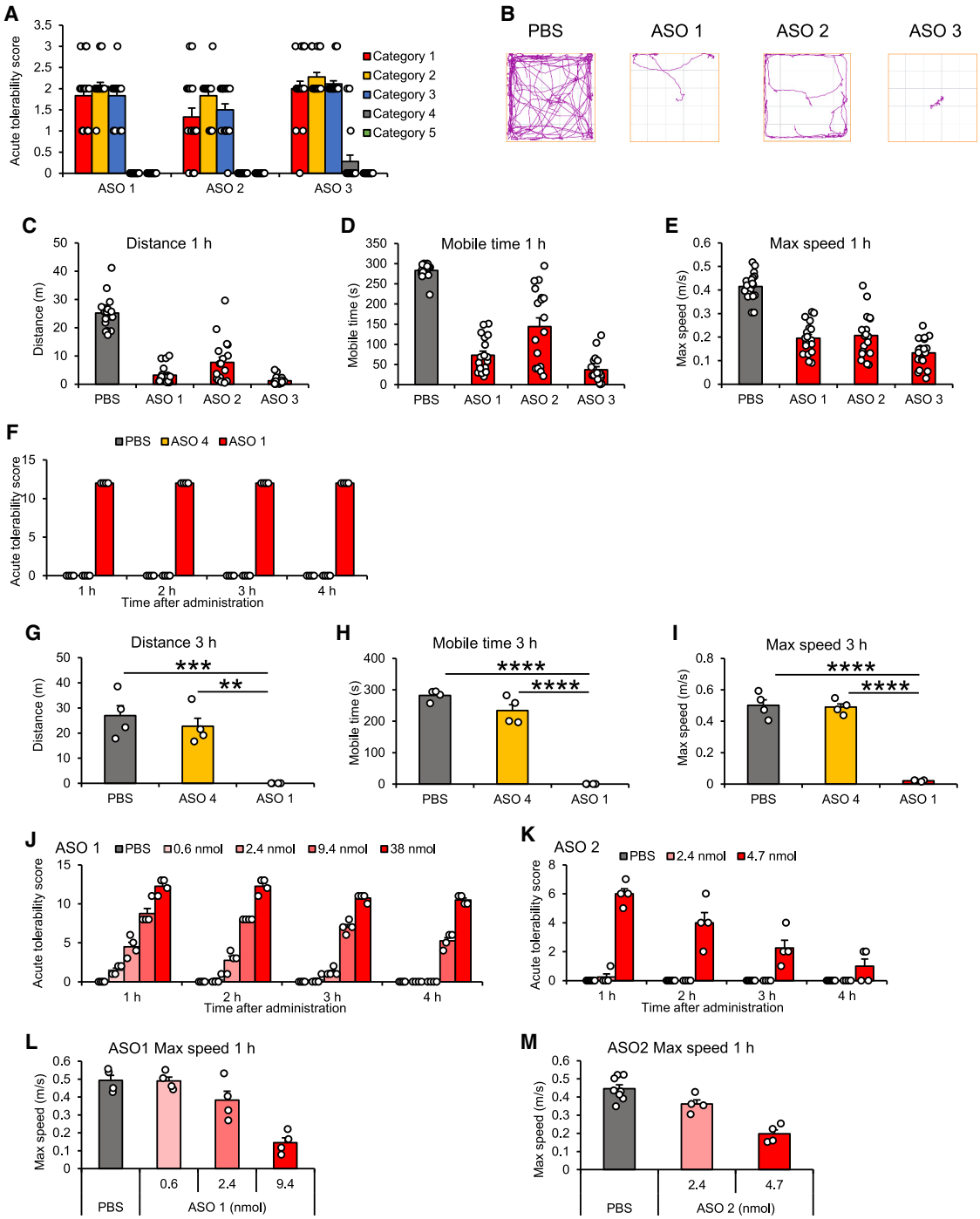

Figure 2. ASOs induce hypoactive neurotoxicity following i.c.v. administration in a dose-dependent manner

(A) Acute tolerability score in each category of mice at 1 h after i.c.v. injection with one of three types of toxic ASO: 2.4 nmol ASO1 (13 μg), 4.7 nmol ASO2 (34 μg), and 2.8 nmol ASO3 (13 μg). (B) Representative track plots of mice shown in (A) at 1 h after administration of ASO or PBS (negative control) in open-field tests. (C–E) Locomotor activity of mice injected with ASOs was assessed in the open-field tests. The three selected parameters were total distance traveled (C), mobile time (D), and maximum speed (E); the mice tested in (A) were also tested in (C)–(E) at 1 h after injection. An automated image analysis system was used to collect data from five independent experiments. (F) Acute tolerability scores in mice after injection of PBS, 38 nmol ASO1 (200 μg), or 38 nmol ASO4. (G–I) Locomotor parameters including distance traveled (G), mobile time (H), and maximum speed (I) of mice shown in (F) at 3 h after administration in open-field tests. (J and K) Dose-response analysis of acute tolerability scores in mice injected with

(legend continued on next page)

and S1). These findings by behavior tests indicate that the *in vivo* phenotypic profiles of neurotoxicity are similar for all tested ASOs, and that these profiles include diminished consciousness and locomotor activity. We next tested a non-toxic ASO, ASO4, which was reported by Hagedorn et al.[14] (Table S1), as a negative control ASO using our behavior tests. No neurotoxicity according to ATSS and open-field tests was observed at any time point in mice administrated 38 nmol ASO4 or PBS (Figures 2F–2I). These results indicate that these analyses are useful for assessing the severity of the neurotoxicity induced by ASOs in mice.

Based on a dose-response study of the CNS toxicity profiles of ASOs, a 1.4- to 3.0-fold increase in the acute tolerability score was detected when 4-fold more ASO1 was injected into mice (Figure 2J); when the dosage of ASO2 was doubled in mice, there was an 11-fold higher acute tolerability score at 1 h after injection and the recovery period was longer (Figure 2K). In open-field tests with three doses of ASO1 or two doses of ASO2, all three parameters of locomotor activity decreased in a dose-dependent manner (Figures 2L, 2M, and S2), which is correlated with an increase in the acute tolerability score. We next assessed recovery time of neurotoxicity induced by the ASOs. Consequently, acute tolerability score of mice injected with 38 nmol ASO1 (200 μg) decreased over time, reaching zero at 17 h after i.c.v. injection (Figure S3A). In addition, decreases in locomotor activity in the open-field test of mice with 38 nmol ASO1 (200 μg), 4.7 nmol ASO2 (34 μg), and 2.8 nmol ASO3 (13 μg) showed recovery to the same level as the PBS-treated group at 12–17, 3, and 7 h, respectively, after the injection (Figures S3B–S3J). These findings demonstrated that the ASO-induced CNS toxicity increased in a dose-dependent manner and is transient, with full recovery within 1 day after the i.c.v. injection.

We next investigated sex and strain difference of neurotoxicity induced by the ASOs using our behavioral analyses. Male mice showed significantly higher acute tolerability scores than that in female mice that had comparable body weight (Figure S4A). Open-field tests also showed that locomotor activity of the male mice decreased more than that of the female mice, although the difference was not significant (Figures S4B–S4D). In addition, we compared neurotoxicity among three different strains of mice using ASO1. Acute tolerability scores were not significantly different in the three strains of female mice with comparable body weight (Figure S5A), but locomotor activity in the open-field tests illustrated that ASO-induced neurotoxicity in C57BL/6J mice was higher than that in Crlj: CD1 (ICR) mice (Figures S5B–S5G). These findings indicate that ASO-induced neurotoxicity in mice is dependent on differences in both sex and mouse strain.

ASO decreases intracellular free calcium levels in primary neuron culture

A previous study of primary cortical neurons *in vitro* demonstrated toxic ASOs reduce spontaneous calcium oscillations.[14] Accordingly, we assumed that calcium transport, which is essential for maintaining cell physiology, may mediate the toxicity of ASOs. To address this issue, we investigated the effect of toxic ASOs on intracellular free calcium levels *in vitro* using rat primary neurons. After treating days 11 *in vitro* (DIV11) primary cortical neurons with toxic ASOs, we measured the intracellular free calcium levels in neurons loaded with a calcium indicator, Fluo-4. In agreement with a previous study, this calcium assay demonstrated that treatment with ASO1–3 treatments lowered intracellular free calcium levels by 3.8%–13.8%; in contrast, the decrease induced by non-toxic ASO4 was up to 3.4%, when compared with CSF-only treatment as a negative control (Figure 3A) in a dose-dependent manner (Figure 3B). These findings demonstrated that toxic ASOs decrease intracellular free calcium levels in neurons.

Effect of ASO oligonucleotide sequence and modifications on neurotoxicity

To investigate the effect of ASO sequence on acute neurotoxicity in mice, we designed new ASOs that had scrambled sequences of ASO1–3, respectively (Table S1). A previous study by Hagedorn et al.[14] reported that the number of G nucleotides and distance between the nearest G nucleotide to the 3′ end both significantly influence calcium oscillation of neurons, which is associated with neurotoxicity of ASOs. The G nucleotide-free stretch in the scrambled ASO1 was markedly longer than the original ASO1, while comparable G nucleotide-free stretches were observed between original ASO2, ASO3, and their scrambled sequences (Figure 4A). After treatment of primary cortical neurons with ASO1–3 and corresponding scrambled sequences, the original ASO1 decreases intracellular free calcium levels more greatly than the scrambled ASO1 (Figure 4B). In contrast, intracellular free calcium levels were comparable among ASO2, ASO3, and ASOs with corresponding scrambled sequences (Figure 4B). Mice injected with the ASO with a scrambled sequence of ASO1 showed lower neurotoxicity than ASO1 with an original sequence in both ATSS evaluation and open-field tests (Figures 4C and S6A–S6C). On the contrary, ASOs with scrambled sequences of ASO2 and ASO3 induced comparable neurotoxicity compared with the ASOs with original sequence (Figures 4D, 4E, and S6D–S6I). These findings corroborate a previous study of the relationship between G position in ASO and the neurotoxic effects of ASO. To assess the effect of chemical modifications in ASO on its neurotoxicity, we next designed ASOs with different chemical modifications in nucleotide or backbones of the ASOs (Table S1). For all three

PBS (J and K), four different doses of ASO1 (J), or two different doses of ASO2 (K). (L) Analysis of maximum speed in mice administrated PBS or varying doses of ASO1 at 1 h after administration in open-field tests. (M) Analysis of maximum speed of the mice shown in (K) at 1 h after administration in open-field tests. Data in (J) were obtained from three independent experiments; data in (K) and (M) were obtained from two independent experiments. Data are represented as mean values ± SEM (A and C–E: n = 18; F–J and L: n = 4; K and M: n = 8 for PBS group, n = 4 for ASO groups). **p < 0.01, ***p < 0.001, ****p < 0.0001; data were analyzed using one-way ANOVA followed by Tukey's post hoc test.

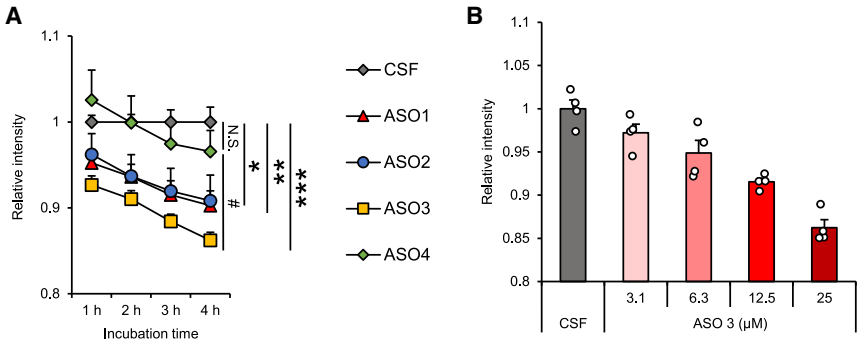

Figure 3. ASOs reduce intracellular free calcium levels in rat primary neurons

(A) Relative intensity levels of Flou4 dye in rat primary cortical neurons after treatment with 25 μM of four types of ASO. *p < 0.05, **p < 0.01, and ***p < 0.001 (CSF versus ASOs) by paired t test; #p < 0.05 (ASO3 versus ASO4) by one-way ANOVA followed by Tukey's post hoc test. (B) Relative intensity levels of Fluo4 in rat primary cortical neurons at 4 h after treatment with four different doses of ASO3. The intensity levels were normalized using a group treated with CSF (negative control). Data are represented as mean values ± SEM (n = 4). N.S., not significant.

ASOs, 2′-*O*-methoxyethyl (MOE) modifications in the wing portions resulted in the lowest reductions in intracellular calcium levels *in vitro* (Figure 4F). We tested mouse neurotoxicity of the modified ASOs by ATSS evaluation and open-field tests. The exchange from locked nucleotide acid (LNA) or 2′-O-methyl (2′OMe) to MOE modification in the wing portion of ASO1 and ASO3 improved their neurotoxicity, respectively (Figures 4G, 4I, S7A–S7C, and S7G–S7I). In contrast, MOE modification in ASO2 did not improve the neurotoxicity; moreover, 2′OMe modification increased its neurotoxicity compared with LNA modification (Figures 4H and S7D–S7F). In addition, the *in vitro* assay showed that ASOs with phosphorothioate (PS) backbones decreased calcium levels more than ASOs with phosphodiester (PO) backbones (Figure 4J). PO backbones extremely lowered neurotoxicity of all three ASOs compared with PS backbones (Figures 4K–4M and S8). These findings indicate that both oligonucleotide sequence and chemical modifications affect the neurotoxicity of ASO in mice, supporting that this *in vivo* neurotoxicity may be correlated with changes of reductions in intracellular free calcium levels *in vitro*.

Calcium channel activator mitigates the acute CNS toxicity of ASOs

To investigate whether the acute CNS toxicity induced by i.c.v. administrated ASO is associated with calcium dynamics, we evaluated an effect of an L-type calcium channel activator, (S)-(−)-Bay K8644 (Bay), on neurotoxicity induced by ASO. Bay increased intracellular free calcium levels *in vitro* and ameliorated the effects of toxic ASO2 on intracellular free calcium levels in neurons (Figure 5A). To test this effect *in vivo*, we first assessed toxicity of Bay at varying doses (data not shown) and determined the maximum tolerable dose of Bay, 1.3 nmol. We then administered toxic ASO1 with or without 1.3 nmol Bay for a bolus i.c.v. injection into mice and compared neurotoxicity using both the ATSS evaluation and open-field test. The mice injected with Bay in addition to ASO1 showed less neurotoxicity in acute tolerability score (Figure 5B), as well as the locomotor function (Figures 5C–5H), than those injected with only ASO1.

AMPAR antagonist magnifies the acute CNS toxicity of ASOs

To test whether AMPAR, which is one of the receptors regulating calcium influx of neurons, affects also the neurotoxicity of the ASOs, we evaluated neurotoxicity of ASO with pretreatment of an AMPAR antagonist, 2,3-dioxo-6-nitro-1,2,3,4-tetrahydrobenzo[f]quinoxaline (NBQX), before an i.c.v. injection of ASOs. NBQX reduced intracellular free calcium levels (Figure S9). Further, combinatorial treatment with NBQX potentiated decreases in intracellular free calcium levels induced by ASO2 (Figure 6A) and modified ASO5 (Figure S10) previously reported to be neurotoxic (Table S1).[22] Then, we confirmed the maximum tolerated dose, i.e., 13.1 nmol, at which NBQX itself did not induce neurotoxicity according to scoring with the ATSS (Figure S11A) and open-field tests (Figure S12). Acute tolerability scores in mice injected with ASO1 after pretreatment with the tolerated dose of NBQX were higher than those of mice injected with ASO1 after pretreatment with PBS as a negative control (the total acute tolerability score of the NBQX and PBS group at 1 h were 6.8 and 4.8, respectively; Figure 6B; Video S2). Similar increases in acute tolerability scores with NBQX pretreatment also occurred with ASO2 (Figure 6C) and ASO3 (Figure S13A). In the analysis from the open-field tests for these three ASOs, mice pretreated with NBQX showed a greater decrease in locomotor function relative to that of mice pretreated with PBS (Figures 6D and S13B) and an 18.5%–90.9% reduction in movement parameters (Figures 6E–6J and S13C–S13H). In addition, the tolerated dose of NBQX itself did not downregulate the target genes of the tested ASOs (Figure S14), and the knockdown efficiency of ASO1 and ASO2 and the ASO delivery level of ASO3 were not affected by pretreatment with NBQX (Figure S15). These findings indicated that blocking AMPARs worsens ASO-induced CNS toxicity without changing the cellular uptake and silencing activity of the ASOs.

AMPAR agonist mitigates the acute CNS toxicity of ASOs

Next, we investigated whether an AMPAR agonist, L-quisqualic acid (L-Q), could alter ASO-induced neurotoxicity. In a Fluo4 assay using primary cortical neurons, L-Q, an AMPAR agonist (Figure S9A), and CX-546, a positive allosteric modulator of AMPAR (Figure 7B), increased intracellular free calcium levels. Moreover, treatment of neurons with L-Q (Figure 7A) or CX-546 (Figure 7B) ameliorated the effects of ASO2 on intracellular free calcium levels. By testing the toxicity of L-Q at several doses, we determined the maximum

A

Name	Oligonucleotide sequence	Number of G oligonucleotides	G-free stretch from 3′-end
ASO 1	ATAGTCACTCTGGTGA	4	1
Scrambled ASO 1	AGTTGACTGCGCTATA	4	5
ASO 2	GGGTCAGCTGCCAATGCTAG	7	0
Scrambled ASO 2	CGTGGTAAGGCACTCCTGGA	7	1
ASO 3	GTATTGCTGAGGA	5	1
Scrambled ASO 3	AGGTAGAGCTTTG	5	0

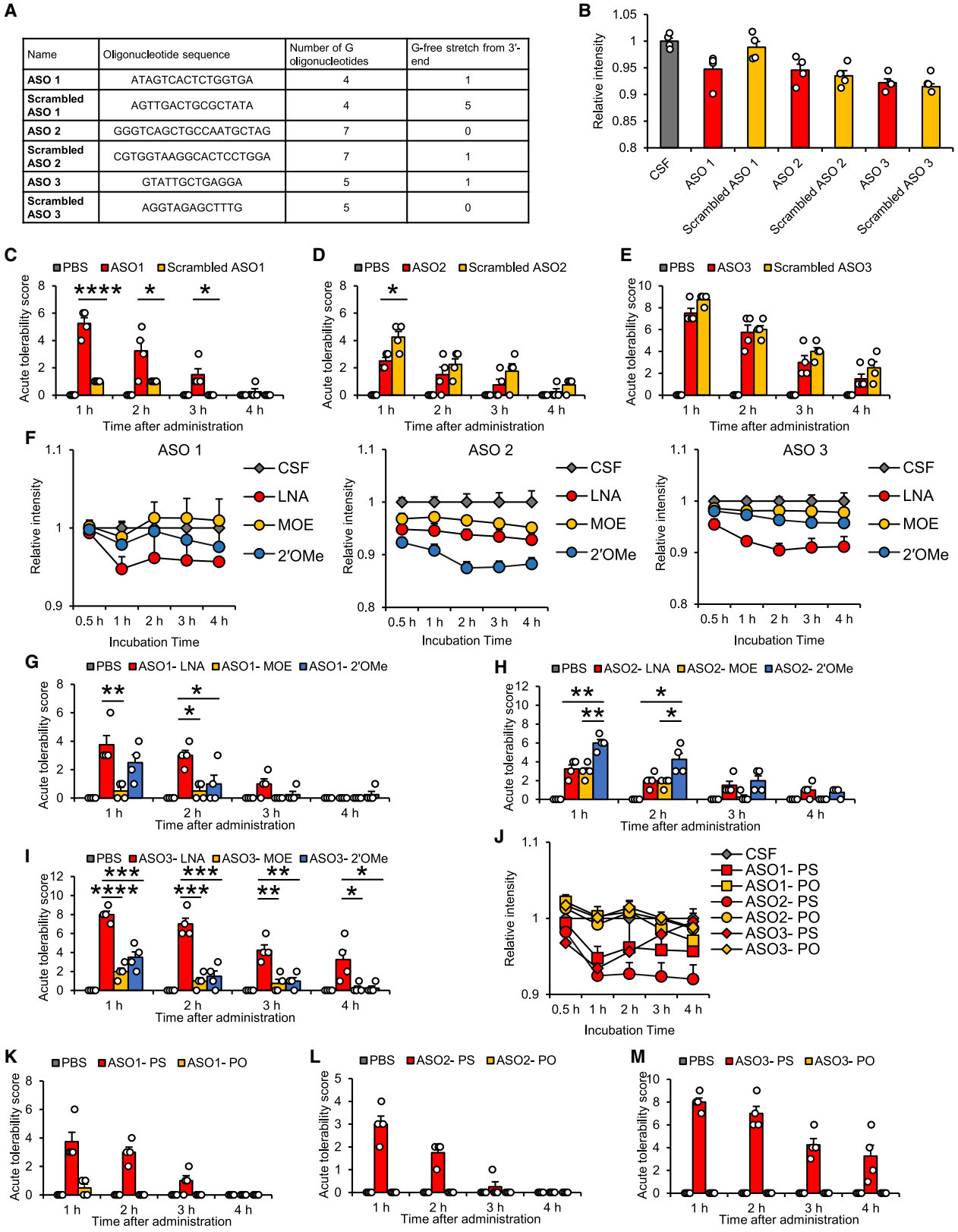

(legend on next page)

tolerated dose at which L-Q slightly induced neurotoxicity with an acute tolerability score of 0.8 ± 0.2 at 1 h after injection (Figure S11B) and did not cause significant disturbance of locomotor function as evaluated in the open-field tests (Figure S12). To explore the effects of L-Q on the acute neurotoxicity of ASOs, we mixed L-Q with these individual ASOs and injected the mixtures into mice via a bolus i.c.v. administration. In contrast with the effects of NBQX, coinjection of L-Q with ASO1 reduced the acute tolerability scores of the mice at every time point by 39.4%–100% compared with the scores of mice injected with ASO1 only (Figure 7C; Video S3). In addition, the gene-silencing effects of the target gene were not affected 1 week after injection (Figure S16A). In the open-field tests, the locomotor activity of the mice treated with additional L-Q was 1.92- to 5.98-fold higher than that of mice treated with ASO1 only at 1 h after i.c.v. injection (Figures 7E and 7G). Also, L-Q showed its mitigating effect on acute tolerability scores of ASO2, which was reduced by 11.8%–54.5% at every time point (Figure 7D). Furthermore, L-Q significantly improved locomotor activity in open-field tests at both 1 h (Figure S17) and 3 h (Figures 7F and 7H) postinjection. Meanwhile, knockdown efficacy of ASO2 was not influenced by L-Q (Figure S16B). Compared with an injection of ASO3 only, coinjection of ASO3 with L-Q reduced acute tolerability score and increased locomotor activity slightly in open-field tests (Figure S18), without reducing ASO delivery levels (Figure S16C).

ASO-induced neurotoxicity is not associated with NMDARs

To investigate whether NMDARs, another main type of inotropic glutamate receptor in neurons, play a role in the acute neurotoxicity of ASO, we used two types of NMDAR antagonist: D-2-amino-5-phosphonopentanoic acid (D-AP5) and dizocilpine (MK801). These two types of NMDAR antagonist did not have a significant effect on intracellular free calcium levels in the neurons (Figure S9B). After determining the maximum tolerated doses of D-AP5 and MK801, i.e., 6.3 and 3.7 nmol, respectively (Figures S11C, S11D, andS12), we injected the antagonists into mice at these doses with an i.c.v. injection of each toxic ASO. Mice administrated with ASO1 showed no significant difference in neurotoxicity with or without either D-AP5 or MK801 pretreatment prior to ASO1 treatment (Figure S19A; Video S4A). Additionally, the NMDAR antagonists had no significant effects on neurotoxicity when administrated simultaneously with ASO1 (Figure S19B; Video S4B). Furthermore, the ASO silencing efficacy at 7 days after injection was not affected by pretreatment (Figure S20A) or coinjection (Figure S20B) with either of the NMDAR antagonists. These findings indicated that NMDARs are not involved in the mechanisms underlying acute ASO-induced CNS toxicity and cellular uptake of the ASOs.

Adding Ca^{2+} to ASO does not mitigate but rather worsens ASO-induced neurotoxicity in mice

ASOs generally have a large number of negative charges linked by phosphorus-based internucleotide linkages. These negatively charged ASOs may chelate positive ions such as Ca^{2+} ions, which causes downregulation of Ca^{2+} levels in the CSF and leads to disrupted calcium homeostasis, which may contribute to abnormal behaviors in mice. Therefore, to test whether the addition of Ca^{2+} ions to ASOs can recover the ASO-induced neurotoxicity, we added Ca^{2+} ions to ASO solutions to reach a final concentration of 10.4 mM, after which we injected the ASO-Ca^{2+} mixture into mice by i.c.v. administration. Unexpectedly, for all three types of ASO, Ca^{2+}-enrichment treatment did not mitigate but rather worsened the neurotoxicity of ASOs (Figures 8A–8C; Figure S21A; Video S5). Additionally, open-field data supported the findings that a high concentration of Ca^{2+} increased the neurotoxicity of ASOs (Figures 8D–8G, S21B–S21E, and S22). At 7 days after injection, for all three types of ASO, target gene levels had no difference between Ca^{2+}-ASO-treated mice and ASO-only-treated mice (Figure S23). These findings indicated that the extracellular addition of calcium to ASO injection could rather exaggerate than improve the neurotoxicity induced by ASOs.

DISCUSSION

In the present study, we determined behavioral characteristics of acute neurotoxicity induced by three types of ASO administered via the i.c.v. route. The identified behavioral abnormalities mainly reflected reduced consciousness and decreased motor function in mice, which occurred in an ASO dose-, sequence-, and modification-dependent manner. Moreover, we revealed four important findings related to the neurotoxicity of ASO *in vivo*. First, toxic ASOs reduce intracellular free calcium levels in an *in vitro* assay, and the decrease is associated with the severity of acute neurotoxicity *in vivo*.

Figure 4. Effect of sequence and modifications on ASO-induced acute neurotoxicity

(A) G nucleotide content of ASO1–3 and corresponding scrambled oligonucleotide sequences. (B) Relative intensity levels of Flou4 dye in rat primary cortical neurons at 1 h after treatment with 25 μM ASO1–3 or corresponding scrambled ASO sequences. (C) Acute tolerability scores in mice administrated PBS, 2.4 nmol ASO1 (13 μg), or the same dose of ASO with a scrambled ASO1 sequence. (D) Acute tolerability scores in mice administrated PBS, 4.7 nmol ASO2 (34 μg), or the same dose of ASO with a scrambled ASO2 sequence. (E) Acute tolerability scores in mice administrated PBS, 2.8 nmol ASO3 (13 μg), or the same dose of ASO with a scrambled ASO3 sequence. (F) Relative intensity levels of Flou4 dye in rat primary cortical neurons after treatment with 25 μM ASO1–3 or the same sequences with varying modifications. (G) Acute tolerability scores in mice after administration of 2.4 nmol of the original LNA-based, MOE-modified, 2′OMe-modified ASO1 or negative control PBS. (H) Acute tolerability scores in mice after administration of PBS or 4.7 nmol MOE-based, LNA-modified, or 2′OMe-modified ASO2. (I) Acute tolerability scores in mice administrated PBS or 2.8 nmol of the original LNA-based, MOE-modified, or 2′OMe-modified ASO3. (J) Relative intensity levels of Flou4 dye in rat primary cortical neurons after treatment with 25 μM ASO1–3 or the same sequences with PO backbones. (K) Acute tolerability scores in mice after administration of PBS or 2.4 nmol ASO1 with PS or PO backbone. (L) Acute tolerability scores in mice after administration of PBS or 4.7 nmol ASO2 with PS or PO backbones. (M) Acute tolerability scores in mice after administration of 2.8 nmol ASO3 with PS or PO backbones. Intensity levels were normalized using a group treated with CSF (negative control) with the ratio of intensity after treatment to before treatment. Data are represented as mean values ± SEM (n = 4). *p < 0.05, **p < 0.01, ***p < 0.001, ****p < 0.0001; data were analyzed using paired t test.

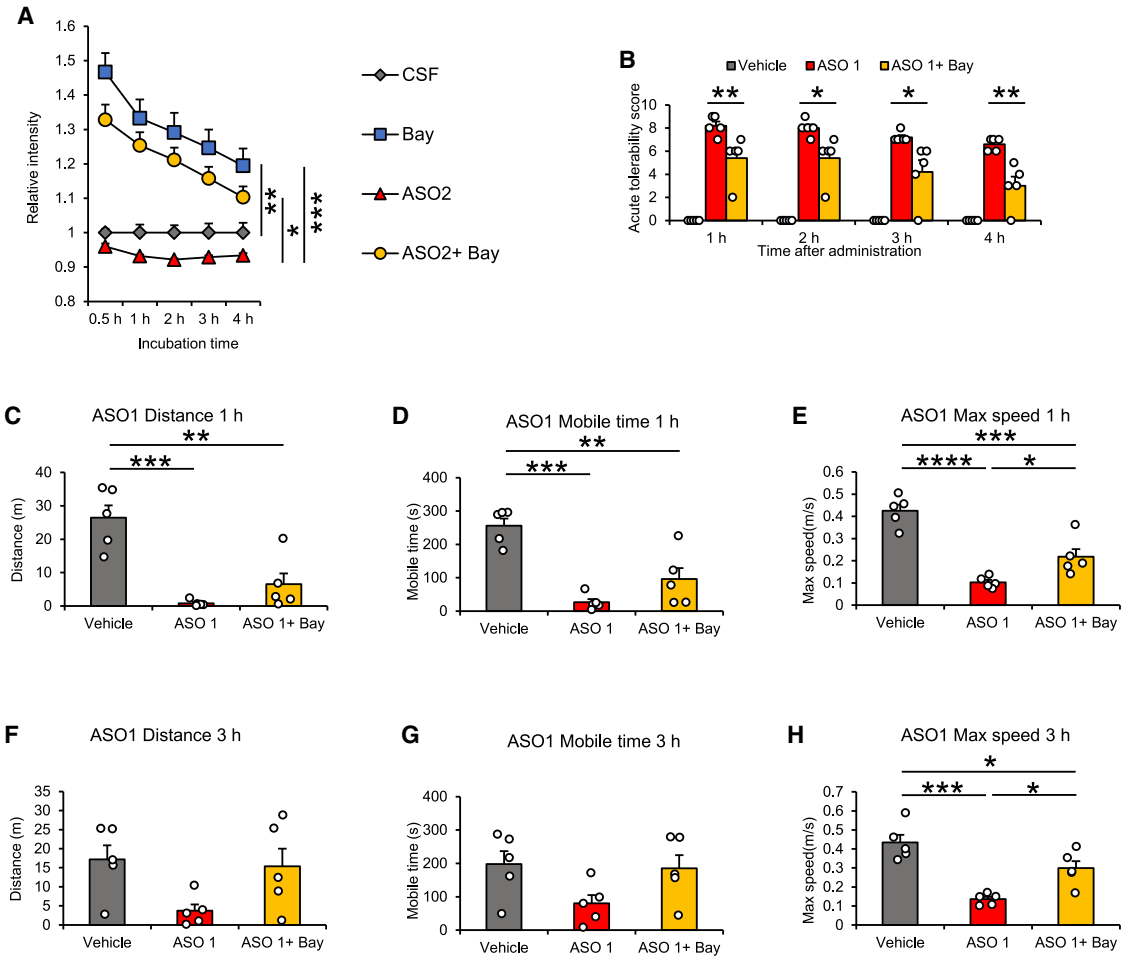

Figure 5. An L-type calcium channel activator, Bay, mitigated acute neurotoxicity of ASO

(A) Relative intensity levels of Flou4 dye in rat primary cortical neurons after treatment with 395 μM Bay, 25 μM ASO2, or combined treatment with both. Intensity levels were normalized to treatment with CSF (negative control). (B) Acute tolerability scores of mice after injection of 2.4 nmol ASO1 (13 μg), ASO1 in addition with 1.3 nmol Bay, or vehicle. (C–E) Locomotor parameters of mice shown in (B) at 1 h after administration in open-field tests. (F–H) Locomotor parameters of mice shown in (B) at 3 h after administration in open-field tests. Data are represented as mean values ± SEM (A: n = 4; B–H: n = 5). *p < 0.05, **p < 0.01, ***p < 0.001, ****p < 0.0001; data were analyzed using paired t test (B) or one-way ANOVA followed by Tukey's post hoc test (A and C–H).

The effects of the modulators on this reduction were consistent with the effects observed during *in vivo* neurotoxicity. Second, the severity of ASO neurotoxicity is reduced by the additional administration of the L-type calcium channel activator and the AMPAR agonist. Third, an antagonist of AMPAR, but not of NMDAR, increased ASO neurotoxicity. Finally, high Ca^{2+} levels in the CSF space also worsen ASO neurotoxicity unexpectedly. Overall, these findings reveal a potential mechanism of ASO neurotoxicity, which is facilitated by regulation of Ca^{2+} level at both extracellular level and intracellular level.

The previous study has shown that ASO can inhibit calcium oscillations in primary neuron cultures *in vitro*[13,14]; hence we investigated the role of extracellular and intracellular calcium ions in ASO neurotoxicity. Because we assumed that negatively charged ASOs may chelate extracellular Ca^{2+} resulting in neurotoxicity, we hypothesized that adding more Ca^{2+} to the CSF would mitigate ASO-induced neurotoxicity. On the contrary, we found that excessive levels of Ca^{2+} worsen the acute neurotoxicity of ASO. This unexpected finding could perhaps be associated with the results of previous studies, i.e., that high extracellular Ca^{2+} levels increase the threshold of activation at AMPARs, resulting in enhanced inhibition of AMPARs by ASOs.[23,24] A previous study demonstrated higher levels of GluA1 and GluA2 in female mice,[25] which may explain the greater neurotoxicity induced by ASO in male mice compared with female mice. In our behavioral analysis, C57BL/6J mice (strain2) showed lower tolerance to ASO neurotoxicity than other strains, which could be explained by the results of a previous report showing that C57 mice were more sensitive to calcium-dependent upregulation of AMPA binding in the hippocampus than other strains.[26] In addition, our *in vitro* analysis using primary neurons showed that toxic ASOs lowered the

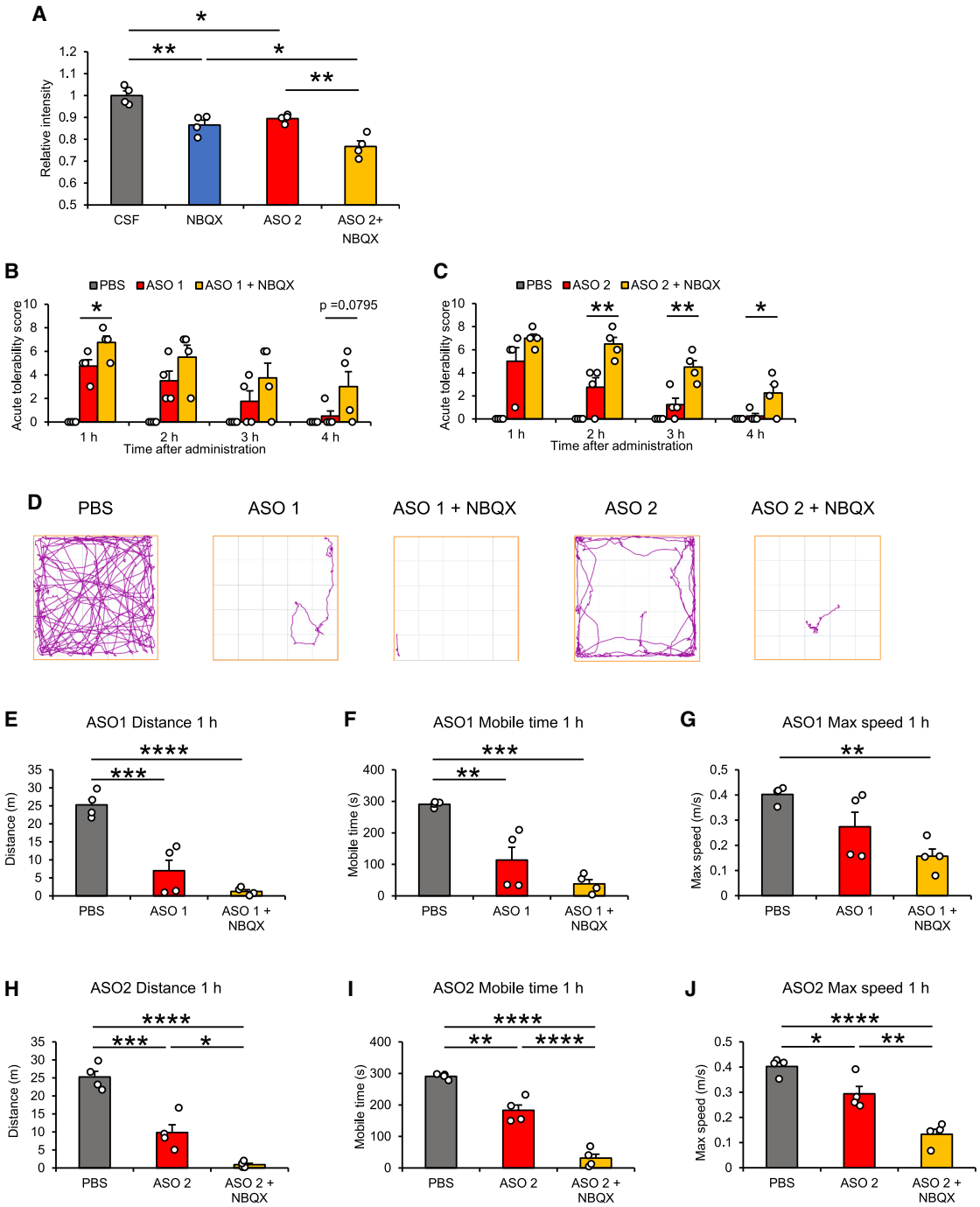

Figure 6. An AMPAR antagonist, NBQX, magnifies the neurotoxicity of ASOs

(A) Intracellular free calcium levels in primary cortical neurons following treatment with 125 μM NBQX, 25μM ASO2, or combined treatment with both. Intensity levels were normalized using a group treated with CSF (negative control). (B) Acute tolerability scores of mice after injection of PBS as a negative control, 2.4 nmol ASO1 (13 μg) with pretreatment of 13.1 nmol NBQX or PBS. (C) Acute tolerability scores of mice after injection of PBS as a negative control, 4.7 nmol ASO2 (34 μg) with a pretreatment of AMPAR antagonist NBQX or PBS. (D) Representative track plots of mice shown in (B) and (C) at 1 h after injection in open-field tests. (E–G) Locomotor parameters of mice shown in (B) at 1 h after injection in open-field tests. (H–J) Locomotor parameters of mice shown in (C) at 1 h after injection in open-field tests. Data are represented as mean values ± SEM (n = 4). *p < 0.05, **p < 0.01, ***p < 0.001, ****p < 0.0001; data were analyzed using paired t test (B and C) or one-way ANOVA followed by Tukey's post hoc test (A and E–J).

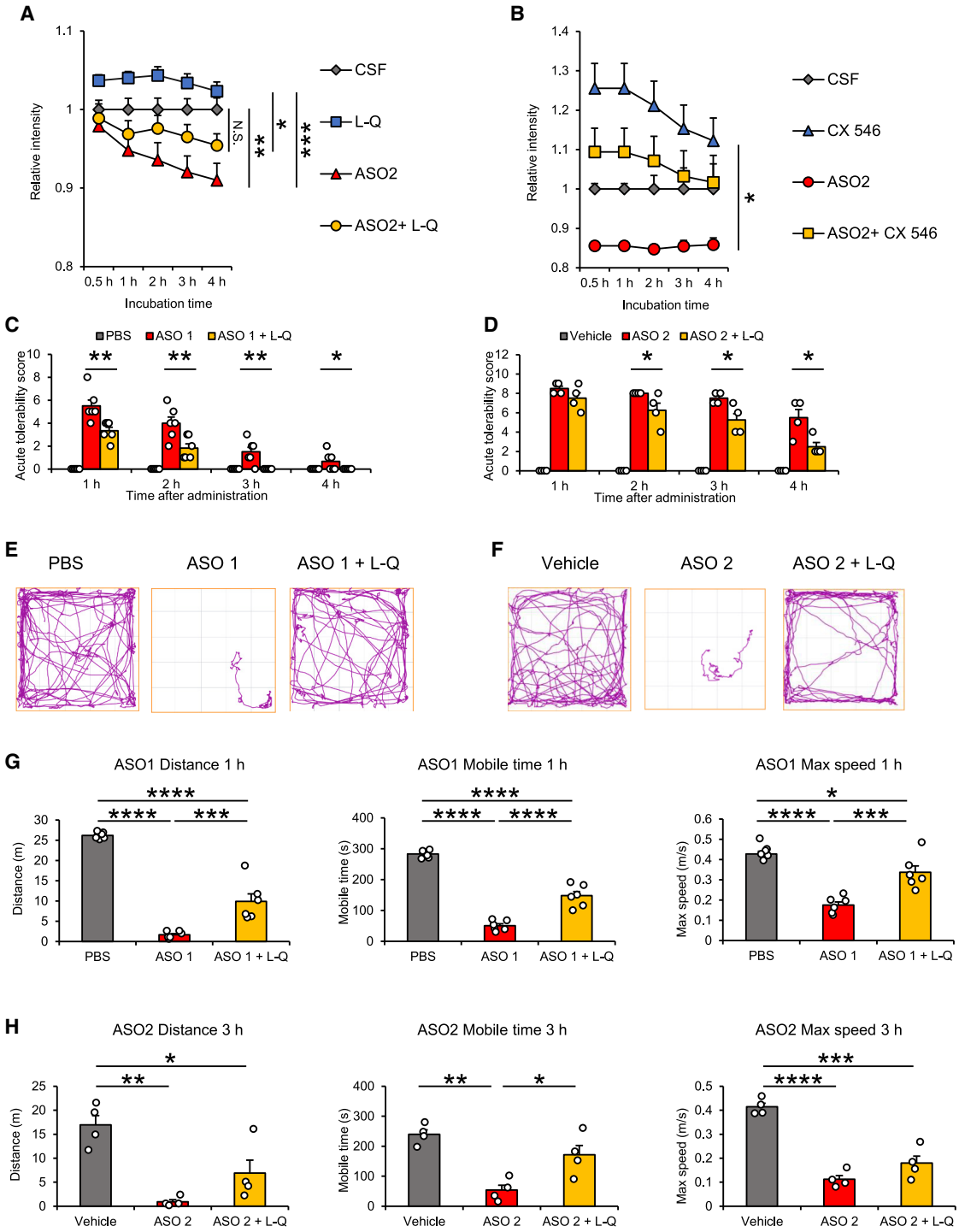

Figure 7. An AMPAR agonist, L-Q, mitigates the acute neurotoxicity of ASOs

(A) Relative intensity levels of Flou4 dye in rat primary cortical neurons after treatment with 800 μM L-Q, 25 μM ASO2, or combined treatment with both. Intensity levels were normalized to treatment with CSF (negative control). (B) Relative intensity levels of Flou4 dye in rat primary cortical neurons after treatment with 5,696 μM CX 546, 25 μM ASO2, or combined treatment with both. Intensity levels were normalized using a group treated with CSF (negative control) with the ratio of intensity after treatment to before treatment. (C) Acute tolerability scores of mice after injection of 2.4 nmol ASO1 (13 μg), ASO1 in addition with 10.6 nmol L-Q, or PBS. (D) Acute tolerability scores of mice after

(legend continued on next page)

intracellular free calcium levels, whereas this decrease was enhanced by the addition of the antagonist of AMPAR and restored by agonists of AMPAR, as well as the L-type calcium channel activator, to increase intracellular free calcium levels in neurons *in vitro* calcium assay. Moreover, these agonists of AMPAR and the calcium channel activator also mitigated neurotoxicity *in vivo*. Thus, although we cannot rule out completely a possibility that the modulators of AMPAR bind directly to the ASOs, the direct modulation of Ca^{2+} intracellular flux seems to be more important than extracellular interaction with Ca^{2+} for the *in vivo* CNS toxicity by ASOs. These findings indicate that promising approaches for clinical application of ASO targeting the CNS include elucidation of calcium-related mechanisms underlying ASO neurotoxicity and development of solution against the toxicity based on its mechanism.

AMPARs and NMDARs are two main ionotropic glutamate receptors on neurons regulating excitatory synaptic transmission in broad areas of the CNS; while the AMPA type mediates faster, the NMDA type mediates more slowly.[27] Given the importance of the physiological maintenance in neural activity by the AMPA and NMDA receptors and considering the characteristics of ASO neurotoxicity based on reduced neuronal activity, we investigated whether AMPARs or NMDARs mediate ASO-induced suppression of *in vivo* neural activity at the acute phase. Additional administration of AMPAR agonists mitigated the neurotoxic effects of ASOs, whereas these effects were exaggerated by administration of an AMPA antagonist. Thus, one hypothesis of possible mechanisms underlying ASO neurotoxicity is inhibition of AMPAR function by ASO, which may decrease intracellular levels of ions, including Na^{+} and Ca^{2+}. This finding is consistent with the results of previous studies, which reported that guanine nucleotides act as competitive glutamate antagonists against AMPARs and thereby reduce intracellular ion levels in neurons.[17,20]

However, further studies that provide evidence of direct binding between ASOs and AMPAR, such as competition assay using AMPAR agonists or antagonists, will be needed to demonstrate the mechanism of AMPAR-dependent ASO neurotoxicity.

The results of the present study demonstrate the effect of ASO sequence and chemical modifications on intracellular free calcium levels, which are associated with acute neurotoxicity severity in mice. Hagedorn et al.[14] demonstrated that the distance between the 3′ end and the nearest guanine nucleotides, G-free stretch, in the ASO sequence influences the effect of ASO on calcium oscillations *in vitro*. Our results of *in vitro* studies indicate the association between G-free stretch and reduction of intracellular free calcium levels, which may be explained by disturbance of neural calcium oscillation. In addition, previous papers reported that chemical modifications influence protein-binding properties of ASOs, subsequently affecting hepatotoxicity of ASOs.[28-31] In particular, PS backbones have stronger binding affinity to proteins compared with PO backbones.[28,29] In contrast, ASOs with MOE modifications bind to proteins weakly compared with other modification, including LNA.[30,31] According to these previous reports, the chemical modifications may alter the binding affinity of ASOs to proteins that regulate calcium transportation in neurons, such as L-type calcium channels and AMPAR, resulting in changes to intracellular free calcium levels.

In our assessment of the silencing effects of ASO on the target genes, none of the modulators had effects on gene expressions and the knockdown efficacy of ASOs. Therefore, the delivery efficiency of ASOs into the CNS is not changed by modulators of glutamate receptor. Consequently, the toxicity mechanism is independent of the major pathway of cellular uptake of ASOs into neurons.

In addition, our analysis of biomarkers, including neuroinflammatory and glial activation markers, showed that both AMPAR antagonist and agonist have no influence on gene expression of those markers after ASO injection (data not shown). These results suggest that the effects of the modulators of AMPAR on the acute neurotoxicity induced by ASO are not explained by the direct binding of the modulators to ASOs.

In summary, we have established a method of behavioral assessment with which to characterize i.c.v. administered ASO-induced CNS toxicity, and we revealed one of the underlying mechanisms, i.e., mediation by Ca^{2+} ions. Based on our findings, we suggest that additional administration of the calcium channel activator or AMPAR agonist can mitigate ASO neurotoxicity without reducing the silencing efficacy of target genes, which is a promising strategy to improve *in vivo* the therapeutic index of ASOs targeting the CNS. Because CNS toxicity of ASOs is one of their crucial limitations for clinical application, our findings could provide new insights to overcome the limitation and make the therapeutic window wider and would lead to the development of novel strategies and technologies for targeting CNS diseases with ASOs.

MATERIALS AND METHODS

Oligonucleotides

The chosen three toxic oligonucleotides with a PS backbone were two DNA/LNA gapmer-type ASOs[32] targeting mouse beta-site amyloid precursor protein cleaving enzyme (*Bace1*) and microtubule-associated protein tau (*Mapt*) mRNAs, respectively, and one 20mer DNA/MOE gapmer-type ASO[33] targeting metastasis-associated lung adenocarcinoma transcript 1 (*Malat1*) long non-coding RNA (as shown in Table S1). ASO1 was reported by Hagedorn et al.[13,14]

injection of vehicle (negative control), 4.7 nmol ASO2 (34 μg) with or without 5.3 nmol L-Q. (E and F) Representative track plots from open-field tests of mice from (C) at 1 h after injection (E) or mice from (D) at 3 h after injection (F). (G and H) Locomotor activity parameters including distance traveled, mobile time, and maximum speed of mice shown in (C) at 1 h after injection (G) and mice shown in (D) at 3 h after injection (H). Data are represented as mean values ± SEM (A, B, D, and H: n = 4; C and G: n = 6). *p < 0.05, **p < 0.01, ***p < 0.001, ****p < 0.0001; data were analyzed using paired t test (C and D) or one-way ANOVA followed by Tukey's post hoc test (A, B, G, and H).

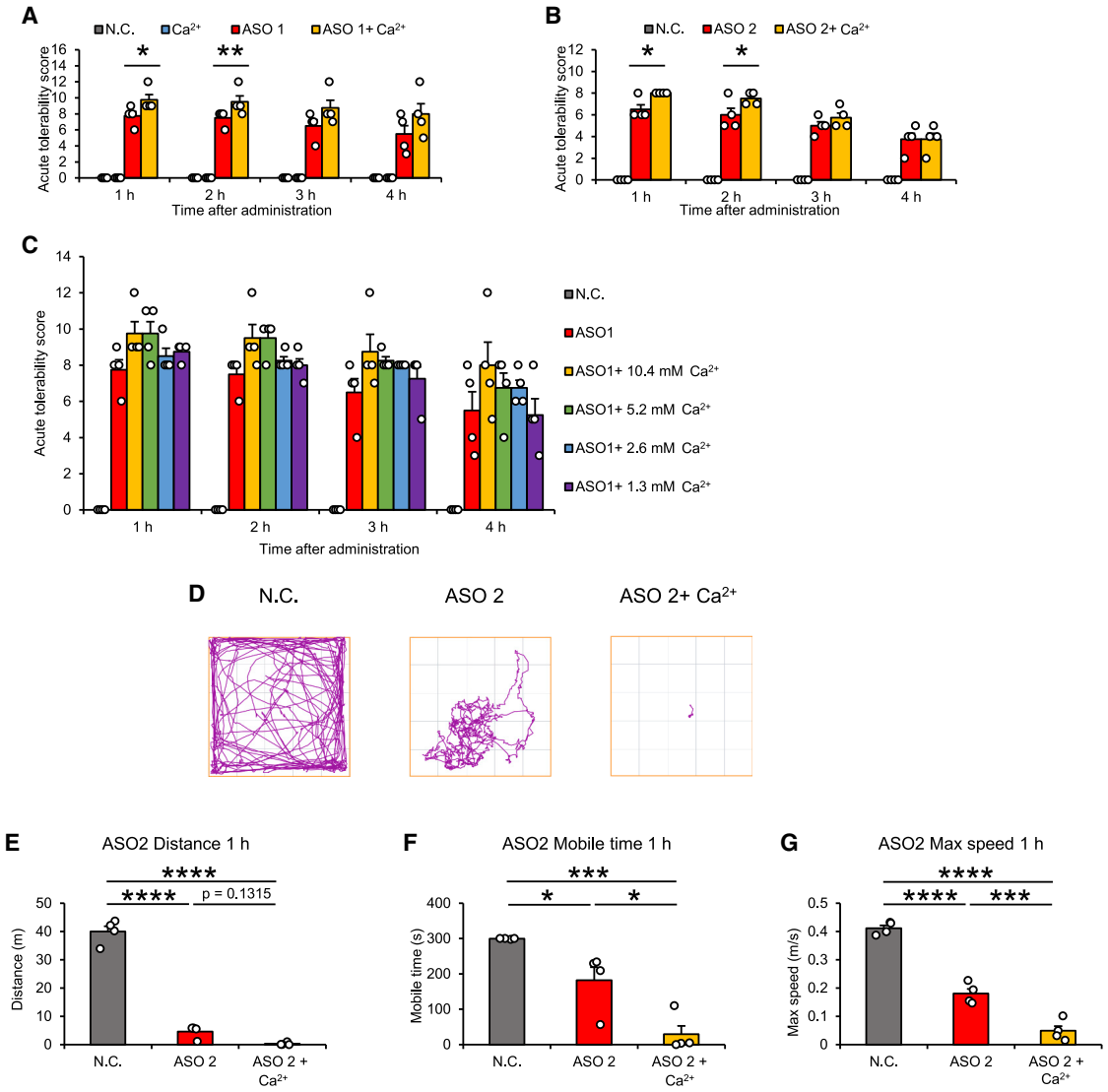

Figure 8. Increase of extracellular Ca^{2+} level does not mitigate but rather worsens the neurotoxicity of ASOs

(A and B) Acute tolerability scores of mice after injection of nuclease-free water as negative control (N.C.), 4.7 nmol ASO1 (25 μg, A) or ASO2 (34 μg, B) with or without 156 nmol Ca^{2+}. (C) Acute tolerability scores in mice after administration of nuclease-free water as a N.C., 4.7 nmol ASO1 only, or 4.7 nmol ASO1 with 156 nmol Ca^{2+}, 78 nmol Ca^{2+}, 39 nmol Ca^{2+}, or 18 nmol Ca^{2+}. (D) Representative track plots of mice shown in (B) at 1 h after i.c.v. injection in open-field tests. (E–G) Three locomotor activity parameters of mice shown in (B) at 1 h after injection in open-field tests. Data are represented as mean values ± SEM (n = 4). *p < 0.05, **p < 0.01, ***p < 0.001, ****p < 0.0001; data were analyzed using paired t test (A and B) or one-way ANOVA followed by Tukey's post hoc test (E–G).

as acutely neurotoxic ASO; on the contrary, ASO4 induced no neurotoxicity with i.c.v. injection into mice. ASO2 and ASO5 with different modifications were also previously reported by Moazami et al.[22] to have acute neurotoxicity in mice. ASO3 was originally designed and tested by our group for silencing *Bace1* by i.c.v. injection into mice.[32] However, we have not yet reported that ASO3 has moderate neurotoxicity at the acute phase. We chose these three ASOs because we elucidate the general mechanisms underlying acute neurotoxicity via the intrathecal (IT) route using these ASOs with different lengths and chemical modifications. All oligonucleotides were synthesized by Ajinomoto (Tokyo, Japan). ASOs were prepared using either nuclease-free water (Invitrogen, Waltham, MA, USA) or 1X PBS (Nacalai Tesque, Tokyo, Japan).

Animals and i.c.v. administrations

All protocols met the ethics and safety guidelines for animal experimentation and were approved by the ethics committee of Tokyo Medical and Dental University (A2021-191A). Animals we used were wild-type female Crlj: CD1 (ICR) mice at 5–7 weeks of age, male Crlj: CD1 (ICR) mice at 4 weeks of age, female C57BL/6J mice at

13 weeks of age, and female BALB/c mice at 12 weeks of age (Oriental Yeast, Tokyo, Japan or Sankyo Labo Service Corporation, Tokyo, Japan). Mice were anesthetized with 2.5% isoflurane and maintained under 2% isoflurane. i.c.v. bolus administrations were performed as previously described[32] with the following modifications. For ASO injection with pretreatment of other reagents, mice were administrated with the modulators at 10 μL/2 min. At 3.5 h after that, oligonucleotides were administrated at 15 μL/3 min through the same burr hole. For the calcium solution, $CaCl_2$ (Nacalai Tesque) was diluted in nuclease-free water at 2.6, 5.2, 10.4, and 20.8 mM, and a final concentration of 1.3, 2.6, 5.2, and 10.4 mM in solution, respectively, was injected into mice. The modulators against glutamate receptors were prepared with PBS buffer using 5 μg (13.1 nmol) of NBQX (Tocris Bioscience, Ellisville, MO, USA) as the AMPAR antagonist, 2 μg (10.6 nmol) or 1 μg (5.3 nmol) of L-Q (Alomone Labs, Jerusalem, Israel) as the AMPAR agonist, 1.3 μg (3.7 nmol) of MK801 (Alomone Labs) as the NMDAR non-competitive antagonist, and 1.3 μg (6.3 nmol) D-2-amino-5-phosphonopentanoic acid (D-AP5) (Alomone Labs) as the NMDAR competitive antagonist; the L-type calcium channel activator was prepared using 0.8 μg (1.3 nmol) of Bay (Tocris Bioscience).

Tolerability evaluation using ATSS

Home-cage neurobehavioral functions were assessed in mice using an ATSS as shown in Figure 1B. In brief, the scale was scored from five categories: (1) consciousness, (2) motor function, (3) appearance, (4) hyperactivity, and (5) involuntary movement. Each category was scaled from 0 to 4. Mice were scored for the severity of CNS side effects on a scale from 0 (no side effects) to 20 (convulsions resulting in euthanasia). ATSS was based on previously described acute tolerability behavioral assessments[13] with several modifications as follows. We defined two new sub-categories with some specific examples of abnormal behaviors in the one category to make clearer and easy-to-use scoring based on the abnormal behaviors that are cross-correlated. Each category score was selected as the higher score in two sub-categories. We arranged the category order as categories 1–3, which show hypoactive behaviors, and categories 4 and 5, which show hyperactive behaviors of mice to help easily follow what kind of abnormal behaviors are in mice after toxic ASO injection. Mice expired during or after i.c.v. administration were scored 22 to score higher than 20, which is the highest score when mice are alive. Animals were observed for changes in their behaviors in the home cage, as well as outside the home cage, i.e., for more detailed observations including measurements of strength and righting response. ATSS evaluation was conducted for each animal following each administrated dose by a separate rater who was blinded from information related to the drug for reliability purposes.

Open-field tests

Mouse locomotor activity was assessed using an open-field test. Mice were placed in the center of an activity field arena, which was a cage (50 cm in width × 50 cm in diameter × 40 cm in height) equipped with a camera above to record activity. Testing lasted for 5 min per animal. The total distance traveled, mobile time, and maximum speed in the open field was analyzed using the ANY-maze video tracking system (Stoelting, Wood Stale, IL, USA).

RNA isolation and quantitative real-time PCR assay

Animal tissue samples were collected at 7 days postdosing. Total RNA was extracted from mouse brain samples using ISOGEN I and following the manufacturer's protocol (Nippon Gene, Tokyo, Japan). cDNA strands were synthesized from total RNA using TAKARA 5× Prime Script RT master mix (Takara Bio, Kusatsu, Shiga, Japan) for use in subsequent quantitative real-time PCR conducted with a LightCycler 480 Probes Master kit (Roche Applied Science, Penzberg, Germany) in a LightCycler 480 instrument (Roche Diagnostics, Mannheim, Germany). A TaqMan MicroRNA Reverse Transcription kit (Applied Biosystem, Foster City, CA) was used to detect ASO3. Primers and probes for ASO3, mouse *Mapt*, and *Bace1* were designed by Applied Biosystems, whereas those for *Malat1* were designed by Sigma-Aldrich. All studies were performed in accordance with Minimum Information for Publication of Quantitative Real-time PCR Experiments (MIQE) guidelines.[34]

Primary neuron culture

Primary neuronal cultures were prepared from the cortices of embryonic day (E) 19 rat embryos from pregnant Crl: CD (SD) International Genetic Standardization (IGS) rats (Oriental Yeast) and collected in cold HBSS+ (Wako, Tokyo, Japan) buffer. Cortical neurons were then isolated using a neuron dissociation solution (Wako) following the manufacturer's protocol, after which they were plated on Corning poly-D-lysine 384-well plates (BioCoat, Horsham, PA, USA) at a density of 15,000 cells/well. Neurons were grown in neuron culture medium (Wako) containing 0.5% penicillin/streptomycin. Primary neuron cultures were incubated at 37°C in a humidified atmosphere 5% CO_2 and 95% air, and the medium was half changed at 4 and 7 days *in vitro*.

Fluo4 calcium assay

Intracellular free calcium levels in primary cortical neurons were detected using the fluorescent Ca^{2+} indicator dye Fluo4 acetoxymethyl ester (Fluo4-AM) with Calcium Fluo4 Kit (Donjindo, Kumamoto, Japan) following the manufacturer's protocol. Primary neuron cultures were loaded with 0.9 μM Fluo4-AM in 25 μL loading buffer, which contains 1X recording buffer supplemented with 5% Pluronic F-127 with a final concentration of 0.04%. Then cultures were incubated at 37°C for 1 h, after which loading buffer was removed and then replaced with 25 μL of human CSF before further incubation with the ASOs or the modulators we used in our study at 37°C for 10 min. Intracellular free calcium levels were measured for 20–50 cycles every 1 s according to the intensity of fluorescent dye at excitation peak: 485 nm/emission peak: 525 nm with a gain of 105–115 using infinite M200 software on TECAN. The modulator against glutamate receptor was prepared using 5,696 μM CX 546 (Tocris Bioscience) as the AMPAR allosteric agonist.

Statistical analysis

Mean values for treatment groups (n = 4, 5, 6, 8, 12, or 18) with corresponding standard errors of the mean were used to plot the figures. Pairwise and multiple comparisons were performed using Student's t tests and one-way ANOVA with Tukey's multiple comparison tests, respectively. Sample group differences with p values <0.05 were considered statistically significant.

DATA AVAILABILITY STATEMENT

The data supporting the findings of this study are available from the corresponding author on reasonable request.

SUPPLEMENTAL INFORMATION

Supplemental information can be found online at https://doi.org/10.1016/j.omtn.2022.12.010.

ACKNOWLEDGMENTS

C.J. would like to thank the Otsuka Toshimi Scholarship Foundation for kindly providing a scholarship (19-S114, 20-S90, 21-S55). This study was supported under grants JP21wm0525032 (to K.Y.) and JP21ae0121026h0001 (to T.Y.) from AMED (Tokyo, Japan), JST FOREST Program (Japan; JPMJFR216H to K.Y.), JSPS KAKENHI Grant-in-Aid for Challenging Research (Exploratory) (JP20K21882) and Scientific Research (B) (JP22H02979) from MEXT (Tokyo, Japan; to K.Y.), and a grant from the Takeda Science Foundation (to K.Y.). The authors would like to thank Enago (http://www.enago.jp) for the English language review.

AUTHOR CONTRIBUTIONS

C.J., S.S.L.M., Y.Y., M.K., and K.Y.-T. performed the experiments and analyzed data. T.Y. and K.Y. conceived and supervised the study. C.J. and K.Y. wrote the manuscript. T.Y. and T.N. reviewed the manuscript.

DECLARATION OF INTERESTS

T.Y. collaborates with Daiichi Sankyo Company, Ltd, Rena Therapeutics, Inc., Takeda Pharmaceutical Company, Ltd, and Toray Industries, Inc., and serves as the academic adviser for Rena Therapeutics, Inc., and Braizon Therapeutics, Inc. All other authors declare no competing interests.

REFERENCES

1. Zamecnik, P.C., and Stephenson, M.L. (1978). Inhibition of Rous sarcoma virus replication and cell transformation by a specific oligodeoxynucleotide. Proc. Natl. Acad. Sci. USA *75*, 280–284.
2. Crooke, S.T., Baker, B.F., Crooke, R.M., and Liang, X.H. (2021). Antisense technology: an overview and prospectus. Nat. Rev. Drug Discov. *20*, 427–453.
3. Gökirmak, T., Nikan, M., Wiechmann, S., Prakash, T.P., Tanowitz, M., and Seth, P.P. (2021). Overcoming the challenges of tissue delivery for oligonucleotide therapeutics. Trends Pharmacol. Sci. *42*, 588–604.
4. Schoch, K.M., and Miller, T.M. (2017). Antisense oligonucleotides: translation from mouse models to human neurodegenerative diseases. Neuron *94*, 1056–1070.
5. Finkel, R.S., Chiriboga, C.A., Vajsar, J., Day, J.W., Montes, J., De Vivo, D.C., Yamashita, M., Rigo, F., Hung, G., Schneider, E., et al. (2016). Treatment of infantile-onset spinal muscular atrophy with nusinersen: a phase 2, open-label, dose-escalation study. Lancet *388*, 3017–3026.
6. Finkel, R.S., Mercuri, E., Darras, B.T., Connolly, A.M., Kuntz, N.L., Kirschner, J., Chiriboga, C.A., Saito, K., Servais, L., Tizzano, E., et al. (2017). Nusinersen versus sham control in infantile-onset spinal muscular atrophy. N. Engl. J. Med. *377*, 1723–1732.
7. Mercuri, E., Darras, B.T., Chiriboga, C.A., Day, J.W., Campbell, C., Connolly, A.M., Iannaccone, S.T., Kirschner, J., Kuntz, N.L., Saito, K., et al. (2018). Nusinersen versus sham control in later-onset spinal muscular atrophy. N. Engl. J. Med. *378*, 625–635.
8. Aartsma-Rus, A. (2021). 'N of 1' therapies need a better model. Nat. Med. *27*, 939.
9. Kim, J., Hu, C., Moufawad El Achkar, C., Black, L.E., Douville, J., Larson, A., Pendergast, M.K., Goldkind, S.F., Lee, E.A., Kuniholm, A., et al. (2019). Patient-customized oligonucleotide therapy for a rare genetic disease. N. Engl. J. Med. *381*, 1644–1652.
10. Crooke, S.T. (2021). A call to arms against ultra-rare diseases. Nat. Biotechnol. *39*, 671–677.
11. Southwell, A.L., Skotte, N.H., Kordasiewicz, H.B., Østergaard, M.E., Watt, A.T., Carroll, J.B., Doty, C.N., Villanueva, E.B., Petoukhov, E., Vaid, K., et al. (2014). *In vivo* evaluation of candidate allele-specific mutant huntingtin gene silencing antisense oligonucleotides. Mol. Ther. *22*, 2093–2106.
12. Toonen, L.J.A., Casaca-Carreira, J., Pellisé-Tintoré, M., Mei, H., Temel, Y., Jahanshahi, A., and van Roon-Mom, W.M.C. (2018). Intracerebroventricular administration of a 2'-O-methyl phosphorothioate antisense oligonucleotide results in activation of the innate immune system in mouse brain. Nucleic Acid Ther. *28*, 63–73.
13. Olson, R.E., Cacace, A.M., Hagedorn, P., Hog, A.M., Nielsen, N.F., LI, D., Brown, J.M., Mercer, S.E., and Jensen, M.L. (2016). W.I. In Methods of Selecting Therapeutic Molecules, Property, Organization, and I. Bureau., ed.. G01N 33/50 (2006.01) ed.
14. Hagedorn, P.H., Brown, J.M., Easton, A., Pierdomenico, M., Jones, K., Olson, R.E., Mercer, S.E., Li, D., Loy, J., Høg, A.M., et al. (2022). Acute neurotoxicity of antisense oligonucleotides after intracerebroventricular injection into mouse brain an be predicted from sequence features. Nucleic Acid Ther. *32*, 151–162.
15. Sharif, N.A., and Roberts, P.J. (1981). Regulation of cerebellar l-[3H]glutamate binding: influence of guanine nucleotides and Na+ ions. Biochem. Pharmacol. *30*, 3019–3022.
16. Monahan, J.B., Hood, W.F., Michel, J., and Compton, R.P. (1988). Effects of guanine nucleotides on N-methyl-D-aspartate receptor-ligand interactions. Mol. Pharmacol. *34*, 111–116.
17. Baron, B.M., Dudley, M.W., McCarty, D.R., Miller, F.P., Reynolds, I.J., and Schmidt, C.J. (1989). Guanine nucleotides are competitive inhibitors of N-methyl-D-aspartate at its receptor site both *in vitro* and *in vivo*. J. Pharmacol. Exp. Ther. *250*, 162–169.
18. Souza, D.O., and Ramírez, G. (1991). Effects of guanine nucleotides on kainic acid binding and on adenylate cyclase in chick optic tectum and cerebellum. J. Mol. Neurosci. *3*, 39–45.
19. Gorodinsky, A., Paas, Y., and Teichberg, V.I. (1993). A ligand binding study of the interactions of guanine nucleotides with non-NMDA receptors. Neurochem. Int. *23*, 285–291.
20. Dev, K.K., Roberts, P.J., and Henley, J.M. (1996). Characterisation of the interaction between guanyl nucleotides and AMPA receptors in rat brain. Neuropharmacology *35*, 1583–1593.
21. Mendieta, J., Gago, F., and Ramírez, G. (2005). Binding of 5'-GMP to the GluR2 AMPA receptor: insight from targeted molecular dynamics simulations. Biochemistry *44*, 14470–14476.
22. Moazami, M.P., Rembetsy-Brown, J.M., Wang, F., Krishnamurthy, P.M., Weiss, A., Marosfoi, M., King, R.M., Motwani, M., Gray-Edwards, H., Fitzgerald, K.A., et al. (2021). Quantifying and mitigating motor phenotypes induced by antisense oligonucleotides in the central nervous system. Preprint at bioRxiv. https://doi.org/10.1101/2021.02.14.431096.
23. Otis, T.S., Raman, I.M., and Trussell, L.O. (1995). AMPA receptors with high Ca2+ permeability mediate synaptic transmission in the avian auditory pathway. J. Physiol. *482*, 309–315.
24. Kumar, S.S., Bacci, A., Kharazia, V., and Huguenard, J.R. (2002). A developmental switch of AMPA receptor subunits in neocortical pyramidal neurons. J. Neurosci. *22*, 3005–3015.

25. Castro-Zavala, A., Martín-Sánchez, A., Montalvo-Martínez, L., Camacho-Morales, A., and Valverde, O. (2021). Cocaine-seeking behaviour is differentially expressed in male and female mice exposed to maternal separation and is associated with alterations in AMPA receptors subunits in the medial prefrontal cortex. Prog. Neuro-Psychopharmacol. Biol. Psychiatry *109*, 110262.

26. Ménard, C., Valastro, B., Martel, M.-A., Martinoli, M.-G., and Massicotte, G. (2004). Strain-related variations of AMPA receptor modulation by calcium-dependent mechanisms in the hippocampus: contribution of lipoxygenase metabolites of arachidonic acid. Brain Res. *1010*, 134–143.

27. Brini, M., Calì, T., Ottolini, D., and Carafoli, E. (2014). Neuronal calcium signaling: function and dysfunction. Cell. Mol. Life Sci. *71*, 2787–2814.

28. Crooke, S.T., Vickers, T.A., and Liang, X.-H. (2020). Phosphorothioate modified oligonucleotide–protein interactions. Nucleic Acids Res. *48*, 5235–5253.

29. Shen, W., De Hoyos, C.L., Migawa, M.T., Vickers, T.A., Sun, H., Low, A., Bell, T.A., 3rd, Rahdar, M., Mukhopadhyay, S., Hart, C.E., et al. (2019). Chemical modification of PS-ASO therapeutics reduces cellular protein-binding and improves the therapeutic index. Nat. Biotechnol. *37*, 640–650.

30. Vickers, T.A., and Crooke, S.T. (2016). Development of a quantitative BRET affinity assay for nucleic acid-protein interactions. PLoS One *11*, e0161930.

31. Liang, X.H., Shen, W., Sun, H., Kinberger, G.A., Prakash, T.P., Nichols, J.G., and Crooke, S.T. (2016). Hsp90 protein interacts with phosphorothioate oligonucleotides containing hydrophobic 2′-modifications and enhances antisense activity. Nucleic Acids Res. *44*, 3892–3907.

32. Lei Mon, S.S., Yoshioka, K., Jia, C., Kunieda, T., Asami, Y., Yoshida-Tanaka, K., Piao, W., Kuwahara, H., Nishina, K., Nagata, T., and Yokota, T. (2020). Highly efficient gene silencing in mouse brain by overhanging-duplex oligonucleotides via intraventricular route. FEBS Lett. *594*, 1413–1423.

33. Hung, G., Xiao, X., Peralta, R., Bhattacharjee, G., Murray, S., Norris, D., Guo, S., and Monia, B.P. (2013). Characterization of target mRNA reduction through *in situ* RNA hybridization in multiple organ systems following systemic antisense treatment in animals. Nucleic Acid Ther. *23*, 369–378.

34. Bustin, S.A., Benes, V., Garson, J.A., Hellemans, J., Huggett, J., Kubista, M., Mueller, R., Nolan, T., Pfaffl, M.W., Shipley, G.L., et al. (2009). The MIQE guidelines: Minimum information for publication of quantitative real-time PCR experiments. Clin. Chem. *55*, 611–622.